



# Potassium permanganate as a promising pre-oxidant to treat low-viability cyanobacteria and associated removal of cyanotoxins and extracellular organic matters

Xi Li<sup>a,b,c</sup>, Jie Zeng<sup>a,b,d</sup>, Xin Yu<sup>e,\*</sup>

<sup>a</sup> Key Lab of Urban Environment and Health, Institute of Urban Environment, Chinese Academy of Sciences, Xiamen 361021, China

<sup>b</sup> University of Chinese Academy of Sciences, Beijing 100049, China

<sup>c</sup> CAS Key Laboratory of Urban Pollutant Conversion, Institute of Urban Environment, Chinese Academy of Sciences, Xiamen 361021, China

<sup>d</sup> Department of Environmental Engineering, Graduate School of Engineering, Kyoto University, Kyoto University Katsura, Nishikyo, Kyoto 615-8540, Japan

<sup>e</sup> College of The Environment & Ecology, Xiamen University, Xiamen, 361102, China

## ARTICLE INFO

### Keywords:

Successive bloom  
Low-viability cyanobacteria  
Potassium permanganate  
Membrane integrity  
Cyanotoxins  
Extracellular organic matters (EOMs)

## ABSTRACT

Cell-viability of cyanobacteria declines from development to decay stage during a successive bloom. Potassium permanganate (KMnO<sub>4</sub>) has demonstrated to be a superior pre-oxidant to treat high-viability cyanobacteria compared to other common oxidants (e.g., chlorine), but whether it is feasible to treat low-viability cyanobacteria is unknown. Here, effects of KMnO<sub>4</sub> on membrane integrity, cyanotoxin fate and extracellular organic matters (EOMs) removal of high- and low-viability cyanobacteria were compared. Results showed that cell-viability of cyanobacteria could affect oxidant decay ( $k_{decay}$ ), membrane damage ( $k_{loss}$ ), and cyanotoxins release ( $k_i$ ) and degradation ( $k_d$ ) during KMnO<sub>4</sub> oxidation, similar to chlorination. However, unlike chlorination, initial low dosages of KMnO<sub>4</sub> (0.5 and 1 mg L<sup>-1</sup>) minimized membrane damage for low-viability cyanobacteria (< 27%), and continuously decrease extracellular cyanotoxins, extracellular organic matters (EOMs), and aromatic compounds to some degrees ( $P < 0.05$ ). High dosages of KMnO<sub>4</sub> (> 2 mg L<sup>-1</sup>) caused severe membrane destruction (> 89%) for low-viability cyanobacteria, leading to a fast increase of extracellular cyanotoxins within 1 h. However, total/extracellular cyanotoxins were oxidized to below the safety guideline of 1 µg L<sup>-1</sup> after being dosed with sufficient oxidant exposure. EOMs and aromatic compounds were also reduced by 5–18% ( $P < 0.05$ ). Additionally, KMnO<sub>4</sub>-assisted coagulation significantly improved the removal of low-viability cyanobacteria (2–5 fold). Consequently, KMnO<sub>4</sub> could be a promising pre-oxidant to treat low-viability cyanobacteria at decay stage of a successive bloom.

## 1. Introduction

Harmful cyanobacterial blooms are proliferating worldwide in natural freshwaters and a range of cyanobacteria species can produce undesirable metabolites (O'Neil et al., 2012; He et al., 2016). Among these metabolites, algal organic matters (AOMs) can be precursor to disinfection by-products (DBPs) and increase coagulant demands in drinking water treatment plants (DWTPs) (He et al., 2016). Moreover, various cyanotoxins have been reported, among which microcystin (MC-LR) is the most studied cyanotoxin. It has been shown to be a potent liver tumor promoter, posing a high risk to human health (Merel et al., 2013). Hence, World Health Organization (WHO) has set a provisional guideline value of 1 µg L<sup>-1</sup> (MC-LR) in drinking water (WHO, 2014).

Conventional water treatment technologies (e.g., coagulation, filtration) can remove a portion of cyanobacteria and intracellular cyanotoxins but are ineffective for extracellular cyanotoxins (Chow et al., 1999; Yap et al., 2014). Pre-oxidation process has been commonly used to enhance cyanobacterial removal and to act as a barrier against extracellular cyanotoxins (Plummer and Edzwald, 2002; Chen and Yeh, 2005; Chen et al., 2009; Ma et al., 2012; Xie et al., 2013; Wang et al., 2013; Fan et al., 2014; Liu et al., 2017). Chlorine, ozone and KMnO<sub>4</sub> are widely employed as pre-oxidants in DWTPs. Previous studies have reported that chlorination and ozonation can easily cause complete cell damage, leading to the release of intracellular cyanotoxins and organic matters (IOMs) even at low dosages (e.g., 1 mg L<sup>-1</sup>) (Daly et al., 2007; Ma et al., 2012; Xie et al., 2013; Zamyadi et al., 2013; Fan et al., 2013b;

\* Corresponding author.

E-mail addresses: [xli@iue.ac.cn](mailto:xli@iue.ac.cn) (X. Li), [jzeng19@hotmail.com](mailto:jzeng19@hotmail.com) (J. Zeng), [xyu@xmu.edu.cn](mailto:xyu@xmu.edu.cn) (X. Yu).

2014; Wert et al., 2014). In contrast, cyanobacteria are less sensitive to  $\text{KMnO}_4$  oxidation, and thus,  $\text{KMnO}_4$  treatments are less likely to result in cell damage and thereby minimize the release of cyanotoxins and EOMs (Xie et al., 2013; Fan et al., 2013a). In addition,  $\text{KMnO}_4$  can oxidize cyanotoxins and AOMs through several reaction pathways including electron exchange, hydrogen abstraction and direct donation of oxygen (Waldemer and Tratnyek, 2006; Rodríguez et al., 2007a; 2007b; Huang et al., 2008; Xie et al., 2013; Li et al., 2014; Kim et al., 2018; Laszakovits et al., 2020). During  $\text{KMnO}_4$  oxidation, adsorption/coprecipitation with newly formed manganese dioxide ( $\text{MnO}_2$ ) can further enhance the removal of cyanobacteria and EOMs by post-coagulation (Chen and Yeh, 2005; Xie et al., 2013; ; Liu et al., 2017; Naceradska et al., 2017). Moreover,  $\text{KMnO}_4$  is useful for controlling the formation of DBPs, tastes and odors in DWTPs (Xie et al., 2013). Therefore, increasing numbers of studies have suggested that  $\text{KMnO}_4$  as a better pre-oxidant to treat cyanobacteria-laden source waters than chlorine or ozone.

To optimize the application of  $\text{KMnO}_4$  to treat cyanobacteria-laden source waters, previous studies have investigated its effects on membrane integrity and associated metabolites (e.g., cyanotoxins, EOMs) removal using high-viability cyanobacteria mainly collected from development stage (Table S1). Nonetheless, in natural freshwaters, cyanobacterial bloom is a successive process, including development, maintenance and decay stages (Tang et al., 2018; Wilhelm et al., 2020). Cell-viability of cyanobacteria declines sharply at decay stage of a successive bloom (Tang et al., 2018; Li et al., 2020a). Li et al., (2020a) found that low-viability cyanobacteria were more susceptible to chlorination attributed to its poor cellular surfaces. During chlorination, cyanotoxins degradation rate of low-viability cyanobacteria decreased due to competitive reactions with EOMs, leading to a high risk of elevated extracellular cyanotoxins (Li et al., 2020a). These results demonstrated that chlorination is not a feasible option for treating low-viability cyanobacteria (Li et al., 2020a). Many studies have shown that  $\text{KMnO}_4$  has a variety of advantages to treat cyanobacteria compared to chlorine, suggesting that  $\text{KMnO}_4$  may be a promising pre-oxidant for low-viability cyanobacteria at decay stage of a successive bloom.

However, to our knowledge, no studies have investigated the effects of  $\text{KMnO}_4$  on membrane integrity and associated metabolites removal of low-viability cyanobacteria. Whether cell-viability of cyanobacteria would affect  $\text{KMnO}_4$  oxidation is also unknown. Consequently, it is strongly essential to compare these effects of  $\text{KMnO}_4$  oxidation on high- and low-viability cyanobacteria. Here, various dosages of  $\text{KMnO}_4$  were employed to treat high- and low-viability cyanobacteria. Oxidant decay, membrane integrity loss, cyanotoxin fate, and EOMs removal were investigated. Then,  $\text{KMnO}_4$ -assisted coagulation experiments were performed to remove high- and low-viability cyanobacteria, with the aim to evaluate the feasibility of  $\text{KMnO}_4$  as a pre-oxidant to treat low-viability cyanobacteria at decay stage of a successive bloom.

## 2. Materials and methods

### 2.1. Materials and reagents

*Microcystis* is one of the most pervasive bloom-forming cyanobacteria in freshwater ecosystems (Harke et al., 2016). In this study, a toxic strain *Microcystis aeruginosa* FACHB-915 was employed to conduct  $\text{KMnO}_4$  experiments. This strain was cultured in BG11 medium (Supporting information Text 1) at 28 °C with a 12 h:12 h light-dark cycle under light intensity of 35  $\mu\text{mol m}^{-2} \text{s}^{-1}$  (Li et al., 2020a).

Potassium permanganate ( $\text{KMnO}_4$ ) stock solution (1.0 g  $\text{L}^{-1}$ ) was standardized by titration with sodium oxalate, and kept under darkness at 4 °C. Sodium thiosulfate stock solution (4.0 g  $\text{L}^{-1}$ ) was employed to terminate oxidative reactions. Polyaluminum chloride (PACl,  $\text{Al}_2\text{O}_3 > 28\%$ , basicity 70–75%) was prepared as a stock solution with a concentration of 1.0 g  $\text{L}^{-1}$ . SYTOX Green nucleic acid stain was purchased from Thermo Fisher Scientific (USA). Microcystin standards (Solarbio, China), methanol, and monopotassium were chromatography grade for

cyanotoxin analysis.

### 2.2. A preparation of high- and low-viability *Microcystis*

A successive *Microcystis* bloom was simulated for 120 d in BG-11 medium, including development, maintenance and decay stages, as described by Li et al. (2020a). Prior to experiments, the same initial cell-density of high and low-viability cells was set to minimize the effects of cyanobacterial biomass on  $\text{KMnO}_4$  oxidation. *Microcystis* samples were collected at 15 d (development stage) and 100 d (decay stage) with the same initial cell-density of approximately  $6.0 \times 10^6$  cells  $\text{mL}^{-1}$ , and monitored using a flow cytometer (Fig. S1). *Microcystis* cells at 100 d held a much lower photosynthetic activity than at 15 d, demonstrating that these samples could well represent high- and low-viability *Microcystis* (Li et al., 2020a) (Fig. S1).

High- and low-viability *Microcystis* were equally diluted with ddH<sub>2</sub>O to a final cell-density of about  $1.0 \times 10^6$  cells  $\text{mL}^{-1}$ , as previous studies have conducted  $\text{KMnO}_4$  experiments to treat high-viability *Microcystis* at development stage with an initial cell-density of  $< 10^6$  cells  $\text{mL}^{-1}$  (Table S1). Adding ddH<sub>2</sub>O did not affect membrane integrity of cyanobacteria, and it did not contain any organic or inorganic matters to affect  $\text{KMnO}_4$  oxidation (Li et al., 2020a; 2020b). This study employed culture solutions as reaction backgrounds, because this culture solution could better show the effects of varied EOMs of high- and low-viability *Microcystis* on  $\text{KMnO}_4$  oxidation.

### 2.3. $\text{KMnO}_4$ oxidation to treat high- and low-viability *Microcystis*

High- and low-viability *Microcystis* were treated with the desired dosages of  $\text{KMnO}_4$  (0.5, 1, 2, 5, 10, or 20 mg  $\text{L}^{-1}$ ) and mixed with a magnetic stirrer at 200 rpm. Magnetic stirring did not impair membrane integrity (Fig. S2). During  $\text{KMnO}_4$  oxidation, *Microcystis* samples were taken at a contact time of 0, 0.2, 0.5, 1, 2, 3, 4, 6, and 8 h. At each time interval, residual  $\text{KMnO}_4$  was measured to establish oxidant decay curves. Furthermore, each sample of 1 mL was taken for membrane integrity analysis. Samples of 100 and 10 mL were immediately quenched with  $\text{Na}_2\text{S}_2\text{O}_3$  and used for cyanotoxins and EOMs analysis, respectively. Control tests were performed using *Microcystis* without adding  $\text{KMnO}_4$ . All of these  $\text{KMnO}_4$  experiments were conducted in 5 L glass conical flasks at the same temperature of  $20 \pm 2$  °C. Influence of pH on cyanotoxin oxidation by  $\text{KMnO}_4$  was negligible (Rodríguez et al., 2007a; Kim et al., 2018), and previous studies have conducted  $\text{KMnO}_4$  experiments for high-viability cells at pH 7–8 (Table S1). Thus, high- and low-viability *Microcystis* samples were adjusted to pH  $7.5 \pm 0.1$  using 0.1 M sodium hydroxide or hydrochloric acid.

### 2.4. $\text{KMnO}_4$ -assisted coagulation to remove high- and low-viability *Microcystis*

High- and low-viability *Microcystis* were prepared as described in Section 2.2. After  $\text{KMnO}_4$  oxidation (0.5, 1, 2, 5, 10, or 20 mg  $\text{L}^{-1}$ ) to treat high- and low-viability *Microcystis* for 1 h, PACl of 10 mg  $\text{L}^{-1}$  was added to *Microcystis* solutions in 1 L glass conical flasks. Control tests were also performed using *Microcystis* without adding  $\text{KMnO}_4$ . *Microcystis* solutions were stirred continuously during coagulation process (400 rpm  $\text{min}^{-1}$ , 1 min; 200 rpm  $\text{min}^{-1}$ , 4 min; 100 rpm  $\text{min}^{-1}$ , 15 min) with six magnetic agitators, and then, solutions were kept motionless for 1 h. Finally, supernatants of *Microcystis* samples were taken for chlorophyll-a measurements using a two-channel fluorometer (AmiScience, USA) and removal ratio of *Microcystis* was estimated.

### 2.5. Gene expression (*mcyH*) of *Microcystis* after $\text{KMnO}_4$ treatment

After  $\text{KMnO}_4$  treatment (0.5 mg  $\text{L}^{-1}$ ; 1 h), high- and low-viability *Microcystis* were collected via centrifugation at  $6000 \times g$  for 5 min (Supporting Information Text 1). These samples were employed to

quantify expression of ABC transporter gene (*mcyH*) via RT-qPCR analysis, since *mcyH* was responsible for transmembrane transport of intracellular microcystin (Tillet et al., 2000; Pearson et al., 2004).

## 2.6. Analytical methods

### 2.6.1. Measurement of $\text{KMnO}_4$ concentration

A standard curve was established by diluting the stock solution of  $\text{KMnO}_4$  (0 to 10  $\text{mg L}^{-1}$ ), and plotted the linear relationship with absorbance at 525 nm (Stewart, 1973; Fan et al., 2013a) (Fig. S3). During  $\text{KMnO}_4$  treatments, residual oxidant was measured by  $A_{525}$  using a UV/VIS spectrophotometer (Thermo Scientific, UK) after filtration with 0.22  $\mu\text{m}$  nylon filters (Millipore, USA) (Fan et al., 2013a). Oxidant concentrations were calculated by a regression equation (Fig. S3).

### 2.6.2. Membrane integrity determination

A flow cytometer (FlowSight, Merck Millipore, USA) was employed for membrane integrity analysis, as described by Li et al. (2020a). SYTOX Green nucleic acid stain can permeate damaged cells and emit a green fluorescence at a fixed wavelength of 488 nm. Prior to FCM analysis, each sample (200  $\mu\text{L}$ ) was incubated for 10 min in darkness after adding SYTOX Green nucleic acid stain with a final concentration of 100 nM. About 10,000 cells were monitored by FCM and these data were analyzed using flow cytometric analysis software (Merck Millipore, USA).

### 2.6.3. Microcystin extraction and quantification

*Microcystis* samples of 50 mL were used for total cyanotoxins quantification. Another volume of 50 mL was centrifuged at 6000 g for 5 min to collect cells for intracellular cyanotoxins quantification (Li et al., 2020a; 2020b). These samples were repeatedly frozen and thawed three times to extract intracellular cyanotoxins. Extracted cyanotoxins were concentrated by C18 solid-phase extraction (SPE) (Nicholson et al., 1994; Li et al., 2020a). A high-performance liquid chromatography (HPLC) system (Agilent 1200, USA) was employed to measure cyanotoxins (Li et al., 2020a; 2020b). Glass vessels were used for cyanotoxins extraction and analysis to avoid the possible adsorption by plastics (Hyenstrand et al., 2001; Altaner et al., 2017).

### 2.6.4. Extracellular organic matter analysis

Dissolved organic carbon (DOC) and UV absorbance at 254 nm ( $\text{UV}_{254}$ ) are common parameters to characterize the amounts of dissolved organic matters and aromatic compounds (Matilainen et al., 2011). *Microcystis* samples of 10 mL were filtered through a 0.45  $\mu\text{m}$  glass fiber membrane (Millipore, USA). DOC was measured by persulfate wet oxidation technique (Shimadzu TOC-V WP).  $\text{UV}_{254}$  of these samples was also measured using a UV3600 Spectrophotometer (Shimadzu, Japan) (Li et al., 2020a).

### 2.6.5. RT-qPCR analysis

RNAs were extracted from *Microcystis* samples via a Spin Column Plant Total RNA Purification Kit (Sangon Biotech, China) (Li et al., 2019a; 2019b). RNAs were transcribed to cDNAs using Synthesis SuperMix (TransGen Biotech, China). cDNAs were used as templates for RT-qPCR analysis performed using a SYBR® Green I qPCR kit (Takara, Japan). Samples were run on an ABI7500 real-time PCR system. Amplification procedures were as follows: initial denaturation 10 min, 95 °C; 35 cycles, 30 s, 95 °C; annealing, 30 s, 50 °C; elongation 30 s, 72 °C (Li et al., 2019a; 2019b).

## 2.7. Statistical analysis

Three parallel  $\text{KMnO}_4$  experiments were conducted. All of the data were statistically analyzed using Student's t-test, and significant difference was defined at  $P < 0.05$ . Statistical analyses were performed using Origin 8.0.

## 3. Results

### 3.1. $\text{KMnO}_4$ decay

$\text{KMnO}_4$  concentration remained constant in BG-11 medium, suggesting that medium components did not cause  $\text{KMnO}_4$  consumption (Fig. 1). With initial high dosages of 10 and 20  $\text{mg L}^{-1}$ , a decay pattern of fast-slow-fast was observed for both high- and low-viability cells (Fig. 1). There was no residual  $\text{KMnO}_4$  after 1–8 h with initial low dosages of 0.5, 1, or 2  $\text{mg L}^{-1}$  for both high- and low-viability cells whereas about 1.5–10.1  $\text{mg L}^{-1}$  was present after 8 h with initial dosages of 5, 10, and 20  $\text{mg L}^{-1}$  (Fig. 1).

To compare  $\text{KMnO}_4$  decay for high- and low-viability cells, a pseudo first-order kinetics model was employed to estimate rate constants ( $k_{\text{decay}}$ ) of oxidant decay according to Eq. (1), as described by Ho et al. (2006) for chlorination:

$$\ln\left(\frac{C_t}{C_0}\right) = -k_{\text{decay}}t \quad (1)$$

where  $t$  (h) = contact time;  $C_t$  ( $\text{mg L}^{-1}$ ) = residual  $\text{KMnO}_4$  concentration after a given contact time;  $C_0$  ( $\text{mg L}^{-1}$ ) = initial  $\text{KMnO}_4$  concentration at  $t = 0$  min; and  $k_{\text{decay}}$  ( $\text{h}^{-1}$ ) = rate constant of  $\text{KMnO}_4$  decay.

Table 1 shows that correlation coefficients ( $R^2$ ) were in the range of 0.94–1.00 and RSS values were much lower than 0.05, demonstrating the good fit of the models. The  $k_{\text{decay}}$  was 0.07–0.61 and 0.10–1.30  $\text{h}^{-1}$  for high- and low-viability cells, respectively (Table 1). Under equal initial dosages of  $\text{KMnO}_4$ ,  $k_{\text{decay}}$  of high-viability cells was higher than that of low-viability cells ( $P < 0.05$ ) (Table 1).

### 3.2. Membrane integrity loss

Prior to  $\text{KMnO}_4$  oxidation, more than 90% of high-viability cells remained intact whereas up to about 55% were damaged for low-viability cells (Fig. 2). Without  $\text{KMnO}_4$  oxidation, there was no membrane destruction of high- and low-viability cells (Fig. 2).  $\text{KMnO}_4$  of 0.5  $\text{mg L}^{-1}$  did not impair membrane integrity for either high- or low-viability cells (Fig. 2). Initial high dosages of 5, 10 and 20  $\text{mg L}^{-1}$  induced complete loss of membrane integrity after a contact time of 2–6 h for high- and low-viability cells (Fig. 2). Moreover,  $\text{KMnO}_4$  at a concentration of 2  $\text{mg L}^{-1}$  resulted in 75% and 89% of membrane damage for high- and low-viability cells, respectively, while lower percentages of 33% and 27% were disrupted with 1  $\text{mg L}^{-1}$ , respectively (Fig. 2).

To compare impairment of membrane integrity of high- and low-viability cells by  $\text{KMnO}_4$  oxidation, rate constants of membrane integrity loss ( $k_{\text{loss}}$ ) were estimated via pseudo first-order kinetics. Eq. (2) below followed Ding et al. (2010):

$$\ln\left(\frac{N_t}{N_0}\right) = -k_{\text{loss}}ct \quad (2)$$

where  $ct$  ( $\text{mg min L}^{-1}$ ) =  $\text{KMnO}_4$  exposure;  $N_t$  ( $\text{cells mL}^{-1}$ ) = cell-density of intact cells after at a specific  $ct$  value;  $N_0$  ( $\text{cells mL}^{-1}$ ) = initial cell-density of intact cells; and  $k_{\text{loss}}$  ( $\text{M}^{-1} \text{s}^{-1}$ ) = rate constant of membrane integrity loss.

Table 2 shows that correlation coefficients ( $R^2$ ) ranged from 0.83–1.00 and RSS values were much lower than 0.05, demonstrating the models fitted well. The  $k_{\text{loss}}$  of high- and low-viability cells was in a range of 3–31 and 10–50  $\text{M}^{-1} \text{s}^{-1}$ , and average  $k_{\text{loss}}$  of low-viability cells was higher than that of high-viability cells ( $P < 0.05$ ) (Table 2). Besides, with the equal initial dosages of  $\text{KMnO}_4$ ,  $k_{\text{loss}}$  of low-viability cells remained higher than that of high-viability cells ( $P < 0.05$ ) (Table 2).

### 3.3. Cyanotoxins release and degradation

With  $\text{KMnO}_4$  at 0.5  $\text{mg L}^{-1}$ , there was a continuous decrease of intracellular and extracellular cyanotoxins without membrane damage

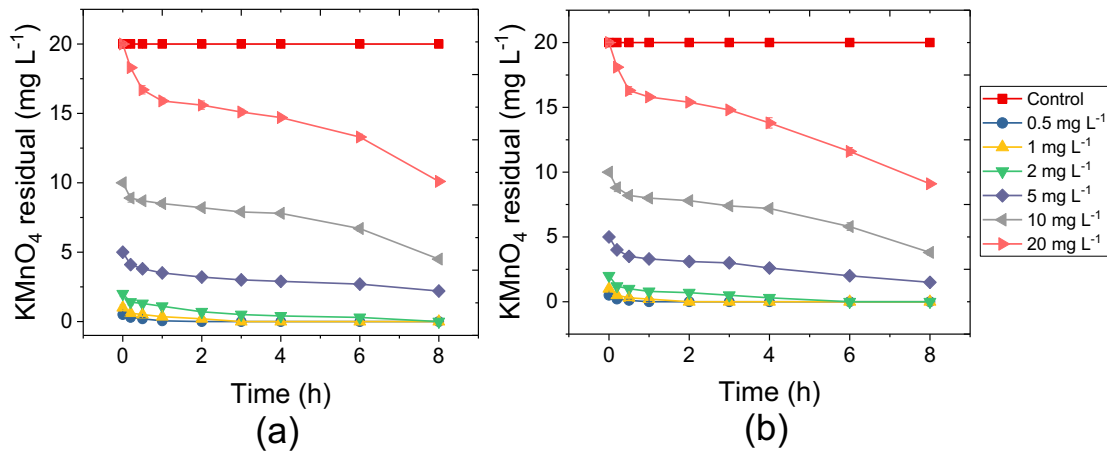


Fig. 1. Residual  $\text{KMnO}_4$  concentrations of high- (a) and low-viability *Microcystis* (b) after initial dosages of 0.5, 1, 2, 5, 10, and 20  $\text{mg L}^{-1}$  to treat high- (a) and low-viability *Microcystis* (b) with a contact time of 0, 0.2, 0.5, 1, 2, 3, 4, 6, and 8 h.

Table 1

Rate constants of  $\text{KMnO}_4$  decay ( $k_{\text{decay}}$ ) of high- and low-viability *Microcystis* treated with various dosages of 0.5, 1, 2, 5, 10, and 20  $\text{mg L}^{-1}$ .

Dosage ( $\text{mg L}^{-1}$ )	High-viability cells				Low-viability cells			
	$k_{\text{decay}}$ ( $\text{h}^{-1}$ )	SE	$R^2$	RSS	$k_{\text{decay}}$ ( $\text{h}^{-1}$ )	SE	$R^2$	RSS
0.5	2.30*	0.38	0.97	$4.70 \times 10^{-2}$	4.08*	/	1.00	/
1	0.61	0.02	1.00	$1.94 \times 10^{-3}$	1.30	0.33	0.94	$3.50 \times 10^{-2}$
2	0.28	0.03	0.96	$2.60 \times 10^{-2}$	0.36	0.03	0.97	$1.90 \times 10^{-3}$
5	0.07	0.01	0.95	$1.50 \times 10^{-2}$	0.12	0.01	0.97	$2.50 \times 10^{-3}$
10	0.08	0.01	0.82	$3.45 \times 10^{-2}$	0.11	0.01	0.81	$4.63 \times 10^{-2}$
20	0.09	0.01	0.88	$4.42 \times 10^{-2}$	0.10	0.01	0.80	$4.09 \times 10^{-2}$

\* and /: values were not accurately estimated due to insufficient data.

SE: standard errors of  $k_{\text{decay}}$ .

$R^2$ : correlation coefficients. RSS: residual sum of squares.

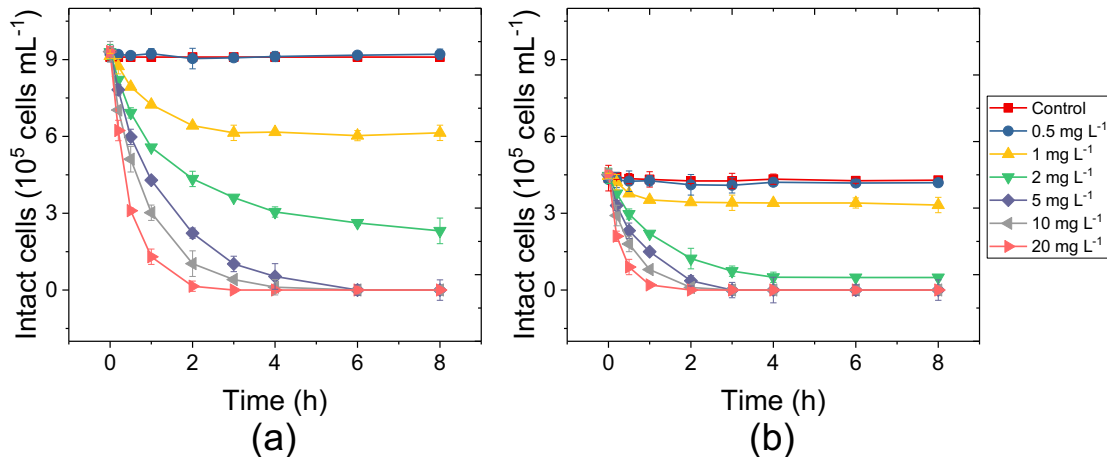


Fig. 2. Cell-density of intact cells of high- (a) and low-viability (b) *Microcystis* treated with initial  $\text{KMnO}_4$  dosages of 0.5, 1, 2, 5, 10, and 20  $\text{mg L}^{-1}$  after a contact time of 0, 0.2, 0.5, 1, 2, 3, 4, 6, and 8 h (For interpretation of the references to color in this figure, the reader is referred to the web version of this article.).

for both high- and low-viability cells ( $P < 0.05$ ) (Fig. 3). Higher initial  $\text{KMnO}_4$  concentrations of 1, 2, 5, 10, and 20  $\text{mg L}^{-1}$  induced membrane damage, leading to the release of intracellular cyanotoxins (Figs. 2 and 3). With an initial dosage of 1  $\text{mg L}^{-1}$ , extracellular cyanotoxins continuously decreased for both high- and low-viability cells ( $P < 0.05$ ) (Fig. 3). However, a pattern of increase-decrease was observed with initial  $\text{KMnO}_4$  of 2, 5, 10, and 20  $\text{mg L}^{-1}$  (Fig. 3). For high-viability cells, extracellular cyanotoxins were degraded to below the safety guideline of 1  $\mu\text{g L}^{-1}$  after 0.5–6 h with an initial  $\text{KMnO}_4$  concentration of 0.5–20  $\text{mg L}^{-1}$  (ct: 96–2718  $\text{mg min L}^{-1}$ ), and a much higher ct ( $> 3312 \text{ mg min L}^{-1}$ ) was required for low-viability cells (Fig. 3).

Cyanotoxins release and degradation were consecutive reactions. Rate constants of intracellular cyanotoxins release ( $k_i$ ) and extracellular cyanotoxins degradation ( $k_e$ ) were estimated by Eqs. (3)–(5) (Fan et al., 2013a; 2014; Li et al., 2020a).

$$\text{MC}_i \xrightarrow{k_i} \text{MC}_e \xrightarrow{k_e} \text{MC}_s \quad (3)$$

$$\text{MC}_i = \text{MC}_{i,0} e^{-k_i \text{ct}} \quad (4)$$

$$\text{MC}_e = \text{MC}_{e,0} e^{-k_e \text{ct}} + \frac{\text{MC}_{i,0} (e^{-k_e \text{ct}} - e^{-k_i \text{ct}})}{1 - k_e/k_i} \quad (5)$$

**Table 2**

Rate constants of membrane integrity loss ( $k_{loss}$ ) of high- and low-viability *Microcystis* treated with initial  $KMnO_4$  dosages of 0.5, 1, 2, 5, 10, and 20  $mg L^{-1}$ .

Dosage ( $mg L^{-1}$ )	High-viability cells				Low-viability cells			
	$k_{loss}$ ( $M^{-1} s^{-1}$ )	SE	$R^2$	RSS	$k_{loss}$ ( $M^{-1} s^{-1}$ )	SE	$R^2$	RSS
0.5	/	/	/	/	/	/	/	/
1	31	3.3	0.91	$5.10 \times 10^{-3}$	50	8.1	0.83	$4.58 \times 10^{-3}$
2	27	2.1	0.96	$2.04 \times 10^{-2}$	43	3.3	0.98	$1.01 \times 10^{-2}$
5	10	0.2	0.99	$1.44 \times 10^{-3}$	17	1.2	1.00	$3.23 \times 10^{-3}$
10	6	0.1	1.00	$1.04 \times 10^{-3}$	10	0.3	1.00	$2.43 \times 10^{-4}$
20	3	0.4	0.93	$4.71 \times 10^{-2}$	9*	0.2	1.00	$1.06 \times 10^{-4}$
Average	15±13				26±19			

/: Values were not estimated, since this treatment did not impair membrane integrity of high- or low-viability cells.

\*: Values were not accurately estimated due to insufficient data.

SE: standard errors of  $k_{loss}$

$R^2$ : correlation coefficients. RSS: residual sum of squares.

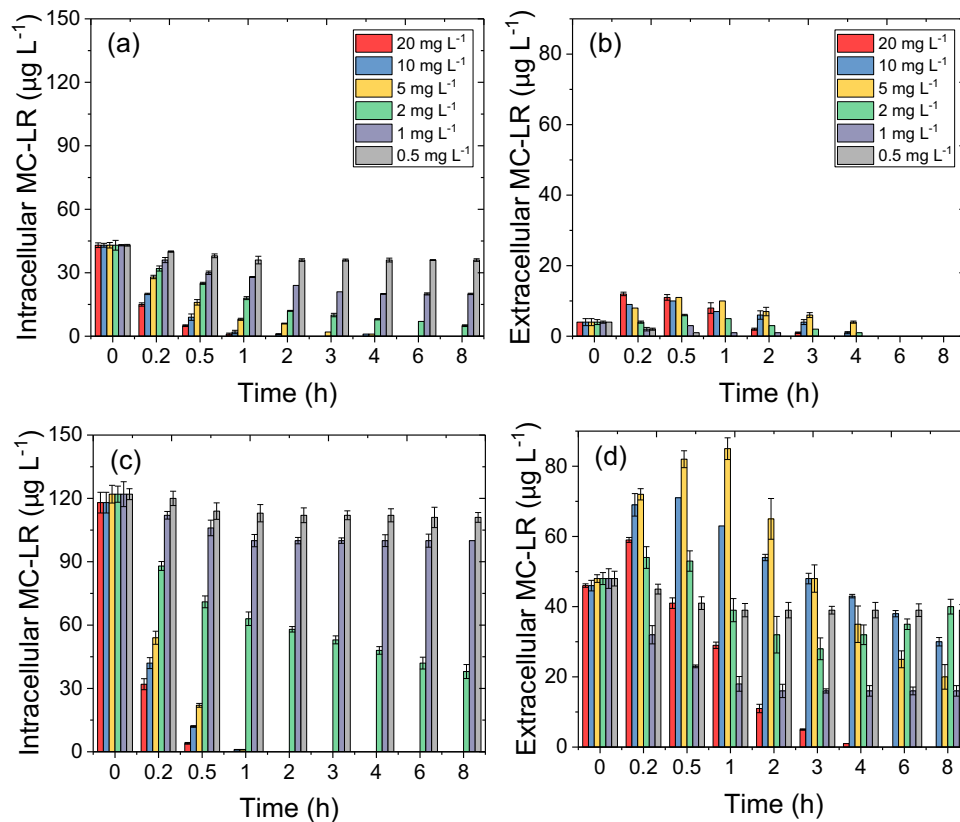


**Fig. 3.** Concentrations of intracellular and extracellular cyanotoxins with initial  $KMnO_4$  dosages of 0.5, 1, 2, 5, 10, and 20  $mg L^{-1}$  with a contact time of 0, 0.2, 0.5, 1, 2, 3, 4, 6, and 8 h. (a): intracellular cyanotoxins of high-viability *Microcystis*; (b): extracellular cyanotoxins of high-viability *Microcystis*; (c): intracellular cyanotoxins of low-viability *Microcystis*; (d): extracellular cyanotoxins of low-viability *Microcystis* (For interpretation of the references to color in this figure, the reader is referred to the web version of this article.).

where  $ct$  ( $mg \text{ min } L^{-1}$ ) =  $KMnO_4$  exposure;  $MC_{i,0}$  ( $\mu g L^{-1}$ ) = initial concentration of intracellular cyanotoxins;  $MC_i$  ( $\mu g L^{-1}$ ) = concentration of intracellular cyanotoxins at a specific  $ct$  value;  $MC_{e,0}$  ( $\mu g L^{-1}$ ) = initial

concentration of extracellular cyanotoxins;  $MC_e$  ( $\mu g L^{-1}$ ) = concentration of extracellular cyanotoxins at a specific  $ct$  value;  $k_i$  ( $M^{-1} s^{-1}$ ) = rate constant of intracellular cyanotoxins release;  $k_e$  ( $M^{-1} s^{-1}$ ) = rate

**Table 3**

Rate constants of intracellular cyanotoxins release ( $k_i$ ) and extracellular cyanotoxins degradation ( $k_e$ ) of high- and low-viability *Microcystis* treated with initial  $KMnO_4$  dosages of 0.5, 1, 2, 5, 10, and 20  $mg L^{-1}$ .

Dosage ( $mg L^{-1}$ )	High-viability cells						Low-viability cells					
	$k_i$ ( $M^{-1} s^{-1}$ )	SE	NSE	$k_e$ ( $M^{-1} s^{-1}$ )	SE	NSE	$k_i$ ( $M^{-1} s^{-1}$ )	SE	NSE	$k_e$ ( $M^{-1} s^{-1}$ )	SE	NSE
0.5	/	/	/	/	/	/	/	/	/	/	/	/
1	40	4.4	0.98	65	8.3	0.89	48	3.1	0.96	56	5.3	0.99
2	41	7.1	0.92	38	5.1	0.98	57	8.2	0.99	23	2.4	0.92
5	21	3.2	0.99	11	1.4	0.88	46	7.4	0.99	8	1.2	0.94
10	17	1.3	0.97	9	0.1	0.95	25*	0.3	0.98	4	1.3	0.81
20	12*	0.4	0.99	6	0.2	0.99	16*	0.5	0.99	3	0.5	0.98

/: Values were not estimated, since this treatment did not cause cyanotoxin release without membrane damage of either high- or low-viability cells.

\*: Values were not accurately estimated due to insufficient data.

SE: standard errors of  $k_i$  and  $k_e$ .

NSE: Nash-Sutcliffe efficiency coefficient.

constant of extracellular cyanotoxins degradation; and  $MC_s$  ( $M^{-1} s^{-1}$ ) = concentration of degraded MC-LR at a specific ct value.

Nash-Sutcliffe efficiency coefficients (NSE) describe the variance of the data that is explained by the model (Mayer and Butler, 1993). If the value is less than 0, this means that the data can not be well explained by the model (Mayer and Butler, 1993). Table 2 shows that NSE ranged from 0.88 to 0.99, suggesting that the model could well describe the data. With equal initial dosages of  $KMnO_4$ ,  $k_i$  ( $46\text{--}57 M^{-1} s^{-1}$ ) of low-viability cells was higher than that of high-viability cells ( $17\text{--}41 M^{-1} s^{-1}$ ), but  $k_e$  ( $4\text{--}56 M^{-1} s^{-1}$ ) was lower than that of high-viability cells ( $6\text{--}65 M^{-1} s^{-1}$ ) ( $P < 0.05$ ) (Table 3). For both high- and low-viability cells,  $k_i$  was lower than  $k_e$  ( $k_i < k_e$ ) with initial  $KMnO_4$  of  $1 mg L^{-1}$ , and an opposite result ( $k_i > k_e$ ) occurred for initial higher dosages of 2, 5, 10 and  $20 mg L^{-1}$  ( $P < 0.05$ ) (Table 3).

### 3.4. Extracellular organic matter removal

For high- and low-viability cells, extracellular DOC and  $UV_{254}$  showed a continuous decrease with initial  $KMnO_4$  of 0.5 and  $1 mg L^{-1}$  ( $P < 0.05$ ) (Fig. 4). In contrast, with initial dosages of 2, 5, 10 and  $20 mg L^{-1}$ , an increase-decrease pattern was observed (Fig. 4). With a sufficient oxidant exposure, DOC and  $UV_{254}$  eventually decreased for both high- and low-viability cells (Fig. 4). Notably, dosages of 2, 5, 10 and  $20 mg L^{-1}$  achieved a higher removal ratio of DOC (16–63%) and  $UV_{254}$  (27–70%) than 0.5 and  $1 mg L^{-1}$  (DOC: 4–18%;  $UV_{254}$ : 14–24%) after a contact time of 8 h ( $P < 0.05$ ) (Fig. 4).

### 3.5. $KMnO_4$ -assisted coagulation to remove high- and low-viability cyanobacteria

Without  $KMnO_4$  oxidation, removal ratios of high- and low-viability cells were about 5% and 20% by PACl coagulation, respectively (Fig. 5). After various dosages of  $KMnO_4$  (0.5, 1, 2, 5, 10, and  $20 mg L^{-1}$ ),

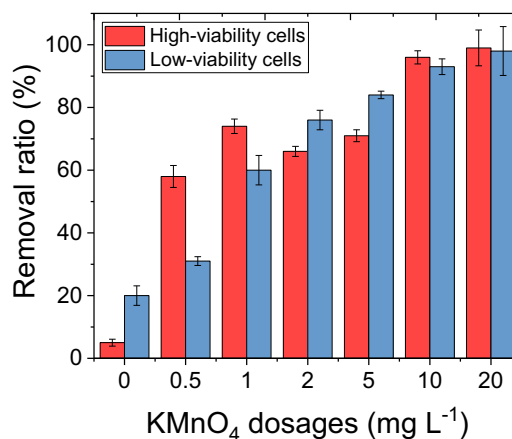


Fig. 5. Removal ratio of high- and low-viability *Microcystis* after  $KMnO_4$ -assisted (0.5, 1, 2, 5, 10, and  $20 mg L^{-1}$ ) coagulation with PACl dosages ( $10 mg L^{-1}$ ).

removal ratios of high- and low-viability cells increased to 58–99% and 31–98% by the same PACl coagulation, respectively ( $P < 0.05$ ) (Fig. 5). Notably, removal ratios of low-viability cells exhibited a positive correlation with initial dosages of  $KMnO_4$ , but removal ratios of high-viability cells were lower with dosages of 2 and  $5 mg L^{-1}$  than that with dosages of 0.5, 1, 10, and  $20 mg L^{-1}$  (Fig. 5).

## 4. Discussion

### 4.1. Effects of cell-viability of cyanobacteria on $KMnO_4$ oxidation

#### 4.1.1. $KMnO_4$ decay

This study found that oxidant decay rate ( $k_{decay}$ ) of low-viability cells

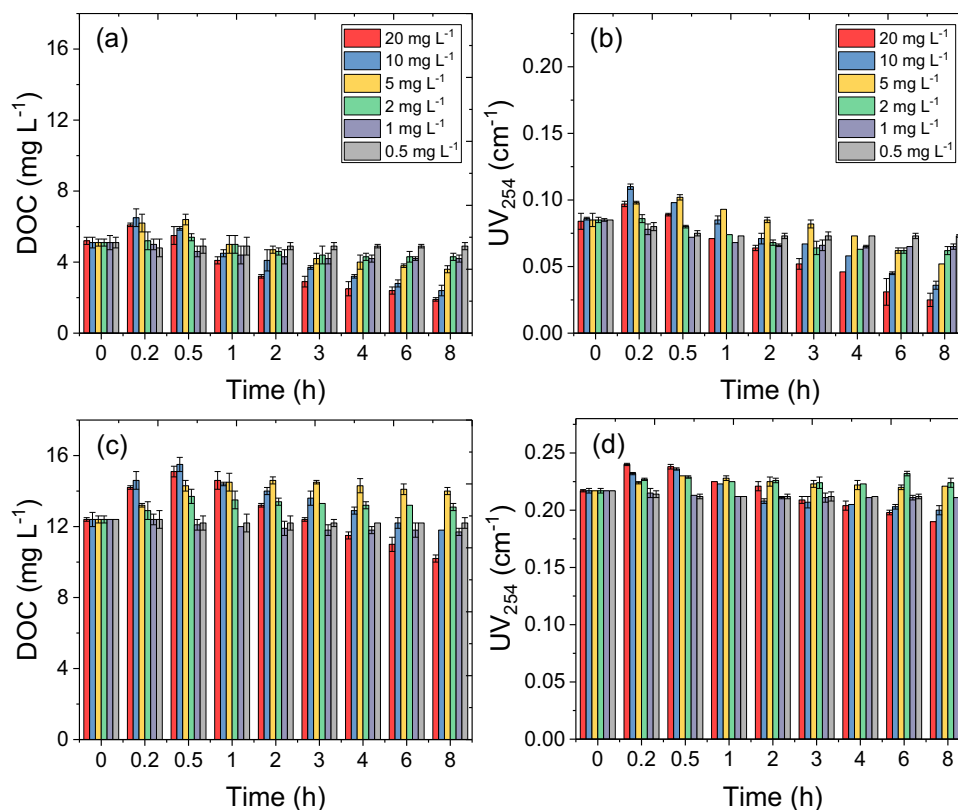


Fig. 4. Concentrations of DOC and  $UV_{254}$  with initial  $KMnO_4$  dosages of 0.5, 1, 2, 5, 10, and  $20 mg L^{-1}$  with a contact time of 0, 0.2, 0.5, 1, 2, 3, 4, 6, and 8 h. (a): DOC of high-viability *Microcystis*; (b):  $UV_{254}$  of high-viability *Microcystis*; (c): DOC of low-viability *Microcystis*; (d):  $UV_{254}$  of low-viability *Microcystis*.

was higher than that of high-viability cells (Table 1). Kim et al. (2018) found that elevated DOC could reduce  $\text{KMnO}_4$  exposure and that  $\text{KMnO}_4$  had high reactivity with aromatic molecules. In this study, low-viability cells exhibited higher concentrations of DOC and  $\text{UV}_{254}$  than high-viability cells ( $P < 0.05$ ) (Fig. 4). Therefore, elevated EOMs containing more aromatic compounds could induce faster  $\text{KMnO}_4$  consumption for low-viability cells than for high-viability cells, the same as for chlorination (Li et al., 2020a).

Cell-viability of cyanobacteria did not affect the pattern of  $\text{KMnO}_4$  decay, and initial high dosages of  $\text{KMnO}_4$  (10 and 20  $\text{mg L}^{-1}$ ) exhibited a decay pattern of fast-slow-fast for both high- and low-viability cells. This result may be ascribed to selective oxidation of AOMs by  $\text{KMnO}_4$ , since Wang et al. (2013) and Kim et al. (2018) reported that  $\text{KMnO}_4$  could effectively oxidize low molecular-weight (MW) AOMs into  $\text{CO}_2$  but showed a lower oxidizing capacity with high-MW proteins and polysaccharides (Jeong et al., 2017; Kim et al., 2018).  $\text{KMnO}_4$  molecules (10 and 20  $\text{mg L}^{-1}$ ) firstly reacted with low-MW EOMs, leading to a fast oxidant decay. Then, the slow decay pattern could be attributed to weaker reaction with high-MW polysaccharides and proteins on cellular surface. After membrane destruction,  $\text{KMnO}_4$  further reacted with the released low-MW IOMs, resulting in a fast oxidant decay.

#### 4.1.2. Membrane integrity loss

Cellular surfaces (e.g., mucilage) are an important barrier to prevent cyanobacteria from oxidant attack. For example, Li et al. (2018) and Xu et al. (2019) observed that *Microcystis* was more resistant to  $\text{KMnO}_4$  attack than filamentous *Pseudoanabaena*, since *Microcystis* had thicker mucilage surrounding cellular surface to form colonies. In this study, low-viability cells exhibited higher rate constants of membrane integrity loss ( $k_{\text{loss}}$ ) than high-viability cells (Fig. 1; Table 2). This result demonstrated that low-viability cells were more susceptible to  $\text{KMnO}_4$  oxidation than high-viability cells, the same as for chlorination (Li et al., 2020a).

In contrast to  $\text{KMnO}_4$ , chlorination held a strong capacity to induce complete membrane destruction of low-viability cells even with initial low dosage of 1  $\text{mg L}^{-1}$  (Li et al., 2020a). However, initial  $\text{KMnO}_4$  of 1  $\text{mg L}^{-1}$  only caused slight membrane damage for low-viability cells (27%), and even, it was slightly lower than high-viability cells (33%) ( $P < 0.05$ ). This result seemed to contradict the conclusion “low-viability cells were less resistant to  $\text{KMnO}_4$  oxidation than high-viability cells.”. Actually, previous studies have noted that membrane destruction mainly depended on oxidant exposure of  $\text{KMnO}_4$  (Fan et al., 2013a; 2013b; Li et al., 2014; Xu et al., 2019). In this treatment, actual oxidant exposure of low-viability cells (11  $\text{mg min L}^{-1}$ ) was much lower than that of high-viability cells (24  $\text{mg min L}^{-1}$ ), and this may have efficiently compensated for their low resistance to  $\text{KMnO}_4$  oxidation. Lower dosage of  $\text{KMnO}_4$  of 0.5  $\text{mg L}^{-1}$  did not disrupt membrane integrity of high- or low-viability cells mainly due to its low reactivity with cyanobacteria. Overall, although low-viability cells were more susceptible to  $\text{KMnO}_4$  attack than high-viability cells, initial low dosages of  $\text{KMnO}_4$  (0.5 and 1  $\text{mg L}^{-1}$ ) as a pre-oxidant could minimize membrane damage to low-viability cells.

#### 4.1.3. Cyanotoxins release and degradation

Kinetics of cyanotoxins release ( $k_i$ ) and degradation ( $k_e$ ) were strongly affected by the changes in cell-viability, similar to results using chlorination (Li et al., 2020a). Low-viability cells exhibited higher  $k_i$ , in line with  $k_{\text{loss}}$  (Tables 2 and 3). Besides,  $k_e$  of low-viability cells was lower than that of high-viability cells (Table 3). Laszakovits and MacKay (2019) found that inhibition of cyanotoxins degradation was ascribed to the competition with dissolved organic matters, and Jeong et al. (2017) reported that the presence of aromatic molecules could exhibit an inhibitory effect on the removal efficiency of cyanotoxins by  $\text{KMnO}_4$  oxidation. Hence, the decrease of  $k_e$  of low-viability cells could be due to its elevated DOC containing more aromatic compounds.

Li et al. (2020a) found that high-viability cells exhibited the pattern

of  $k_e > k_i$  whereas the changed pattern of  $k_e < k_i$  occurred for low-viability cells during chlorination. Unlike chlorination, cell-viability did not affect the pattern ( $k_e > k_i$  or  $k_e < k_i$ ) by  $\text{KMnO}_4$  oxidation, and the pattern only depended on the initial dosages of oxidant for both high- and low-viability cells.  $\text{KMnO}_4$  (1  $\text{mg L}^{-1}$ ) could continuously decrease extracellular cyanotoxins with slight membrane damage for both high- and low-viability cells attributed to the same pattern of  $k_e > k_i$  (Table 3). With initial  $\text{KMnO}_4$  concentrations of 2, 5, 10, and 20  $\text{mg L}^{-1}$ , extracellular cyanotoxins increased within 1 h ascribed to the changed pattern of  $k_e < k_i$  (Table 3). However, extracellular/total cyanotoxins were degraded to below the safety guideline of 1  $\mu\text{g L}^{-1}$  for high-viability cells with a ct value of 96–2718  $\text{mg min L}^{-1}$  whereas a much higher ct ( $> 3312 \text{ mg min L}^{-1}$ ) was required for low-viability cells due to the decrease of  $k_e$  (Fig. 3; Table 3). Moreover,  $\text{KMnO}_4$  of 0.5  $\text{mg L}^{-1}$  continuously degraded extracellular cyanotoxins without membrane damage for both high- and low-viability cells (Fig. 3). These results suggested that  $\text{KMnO}_4$  could effectively decrease the risk of cyanotoxins for both high- and low-viability cells with or without membrane damage.

#### 4.1.4. Mechanism of intracellular cyanotoxin decrease

$\text{KMnO}_4$  (1, 2, 5, 10, and 20  $\text{mg L}^{-1}$ ) induced the loss of membrane integrity, and thus, the decrease of intracellular cyanotoxins could be ascribed to the fast release of intracellular cyanotoxins (Figs. 2 and 3). Furthermore, this study employed SYTOX Green (molecular weight: 509) to determine membrane integrity, since the dye could permeate damaged membrane. Molecular weight of  $\text{KMnO}_4$  (158) is less than SYTOX Green, suggesting that it could permeate damaged cells to degrade intracellular cyanotoxins. Consequently, the two pathways are important to decrease intracellular cyanotoxins for both high- and low-viability cells after  $\text{KMnO}_4$  oxidation caused membrane destruction.

Intriguingly,  $\text{KMnO}_4$  of 0.5  $\text{mg L}^{-1}$  decreased intracellular cyanotoxins for both high- and low-viability cells without membrane destruction (Figs. 2 and 3). A similar result was also observed for high-viability cells by Fan et al. (2013a), but its mechanism was not well understood. Ross et al. (2019) found that exposure to various levels of salinity resulted in the active release of intracellular cyanotoxins without membrane damage via membrane transporters encoded by *mcyH*. Fig. 6 shows that *mcyH* was upregulated of 2.6–3.9 fold for high-viability cells, whereas there was no significant change ( $< 1$ -fold) for low-viability cells. This suggested that  $\text{KMnO}_4$  could accelerate the secretion of intracellular cyanotoxins via transmembrane transporters for high-viability cyanobacteria, but this strategy was not adopted by low-viability cells. Compared with high-viability cells, about 55% of low-viability cells had damaged cellular membranes due to physiological injury after cell aging (Li et al., 2020a). This indicated that the permeation of  $\text{KMnO}_4$  molecules through damaged cellular membranes may be another pathway to decrease intracellular cyanotoxins by

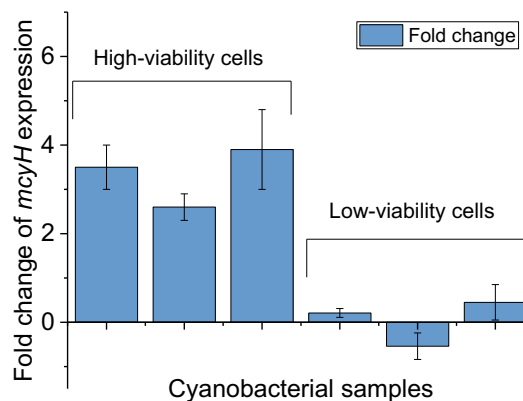


Fig. 6. Fold change of *mcyH* expression of high- and low-viability *Microcystis* treated with  $\text{KMnO}_4$  oxidation (0.5  $\text{mg L}^{-1}$ ; 1 h).

low-viability cells.

#### 4.1.5. Extracellular organic matters (EOMs) removal

At present, there is an argument concerning EOMs removal after  $\text{KMnO}_4$  oxidation to treat cyanobacteria-laden waters. Xie et al. (2013) observed an increase of DOC without membrane damage attributed to  $\text{KMnO}_4$  reactions with surface mucilage. Nevertheless, other studies have demonstrated that  $\text{KMnO}_4$  could oxidize AOMs (MW < 11 kDa) to  $\text{CO}_2$  and that the newly formed  $\text{MnO}_2$  could further remove organic matters via physical adsorption (Wang et al., 2013; Naceradska et al., 2017). In this study,  $\text{KMnO}_4$  (0.5 and 1 mg L<sup>-1</sup>) achieved a continuous decrease of DOC within 1 h, and this was ascribed to three reasons: (1)  $\text{KMnO}_4$  oxidized low-molecule AOMs to  $\text{CO}_2$ ; (2)  $\text{MnO}_2$  adsorption for AOMs; and (3) minimum release of IOMs with slight membrane destruction. Meanwhile, aromatic compounds (UV<sub>254</sub>) continuously decreased in these treatments, in agreement with Naceradska et al. (2017) and Laszakovits et al. (2020). In contrast, with higher dosages of 2, 5, 10, and 20 mg L<sup>-1</sup>, DOC and UV<sub>254</sub> increased for both high- and low-viability cells within 1 h, due to the fast release of IOMs after severe membrane destruction (Figs. 2 and 4). However, with a sufficient oxidant exposure, DOC and UV<sub>254</sub> eventually decreased for both high- and low-viability cells, since these released IOMs could be effectively degraded via  $\text{KMnO}_4$  oxidation. In general,  $\text{KMnO}_4$  held a strong capacity to decrease EOMs/aromatic compounds for both high- and low-viability cells with or without membrane damage.

#### 4.2. Evaluation of $\text{KMnO}_4$ as a promising pre-oxidant to treat low-viability cyanobacteria

Various dosages of  $\text{KMnO}_4$  as a pre-oxidant showed a good performance in enhancing the removal of low-viability cells by PACl coagulation, and its removal ratio was positively correlated with initial dosages of  $\text{KMnO}_4$ . Among these pre-oxidation treatments, low dosages of  $\text{KMnO}_4$  (0.5 and 1 mg L<sup>-1</sup>) could minimize membrane destruction and continuously decrease cyanotoxins and EOMs/aromatic compounds for low-viability cells. However, it must be noted that residual extracellular cyanotoxins were above the safety guideline of 1 µg L<sup>-1</sup> even after a sufficient contact time of 1–2 h, which was mainly attributed to initial elevated cyanotoxins and the decrease of  $k_e$ . Hence, combining with other water treatment processes (e.g., activated carbon adsorption) may be necessary to further remove residual extracellular cyanotoxins for low-viability cells (Ho et al., 2011; Jeong et al., 2017). High dosages of  $\text{KMnO}_4$  (2, 5, 10 and 20 mg L<sup>-1</sup>) induced severe membrane destruction, but sufficient oxidant exposure ( $ct > 3312$  mg min L<sup>-1</sup>) could degrade extracellular cyanotoxins to below the safety guideline of 1 µg L<sup>-1</sup> and achieve the highest removal ratio of EOMs/aromatic compounds among these treatments. Notably, residual oxidant was another important issue in this treatment, since a residual  $\text{KMnO}_4$  of 0.05 mg L<sup>-1</sup> or higher will result in a pink taint of drinking water. Overall, drawbacks and advantages of  $\text{KMnO}_4$  as a pre-oxidant to treat low-viability cyanobacteria should be carefully assessed in practice.

## 5. Conclusions

Although the change in cell-viability could affect  $\text{KMnO}_4$  oxidation to treat cyanobacteria to some extent, this study suggested that  $\text{KMnO}_4$  could be a promising pre-oxidant to treat low-viability cyanobacteria. The main findings are given below:

- (i) Fast-slow-fast pattern of  $\text{KMnO}_4$  decay was not changed by cell-viability of cyanobacteria.
- (ii) Low-viability cyanobacteria were less resistant to  $\text{KMnO}_4$  oxidation than high-viability cyanobacteria, but low dosages of  $\text{KMnO}_4$  (0.5 and 1 mg L<sup>-1</sup>) could minimize membrane damage for low-viability cyanobacteria.

- (iii) Cell-viability of cyanobacteria did not change the pattern of cyanotoxins release and degradation ( $k_e > k_i$  or  $k_e < k_i$ ), and the pattern was only depending on initial dosages of  $\text{KMnO}_4$  for both high- and low-viability cyanobacteria.
- (iv) Without membrane destruction,  $\text{KMnO}_4$  accelerated the secretion of intracellular cyanotoxins via transmembrane transporters for high-viability cyanobacteria, but this strategy was not adopted by low-viability cyanobacteria.
- (v)  $\text{KMnO}_4$  decreased the risk of extracellular cyanotoxins and EOMs/aromatic compounds for both high- and low-viability cyanobacteria with or without membrane destruction.
- (vi) Various dosages of  $\text{KMnO}_4$  as a pre-oxidant enhanced the removal of both high- and low-viability cyanobacteria by PACl coagulation.

## CRedit authorship contribution statement

**Xi Li:** Visualization, Writing – review & editing, Investigation, Data curation, Conceptualization. **Jie Zeng:** Investigation, Writing – review & editing. **Xin Yu:** Funding acquisition.

## Declaration of Competing Interest

The authors declare that they have no known competing financial interests or personal relationships that could have appeared to influence the work reported in this paper.

## Acknowledgments

This work was supported by National Key R&D Program of China (no. 2017YFE0107300), and Science & Technology Major Project of Xiamen (no. 3502Z20171003). Special thanks for a scholarship provided by the University of Chinese Academy of Sciences (UCAS). We are so grateful for the many suggestions that Dr. Olga I. Belykh, Dr. Irina V. Tikhonova, Dr. Sergey A. Potapov, and Dr. Andrey Yu. Krasnopeev improved our manuscript.

## Supplementary materials

Supplementary material associated with this article can be found, in the online version, at doi:10.1016/j.watres.2021.117353.

## References

- Altaner, S., Puddick, J., Dietrich, D., 2017. Adsorption of ten microcystin congeners to common laboratory-ware is solvent and surface dependent. *Toxins* 9 (4), 129.
- Chen, J.J., Yeh, H.H., 2005. The mechanisms of potassium permanganate on algae removal. *Water Res.* 39 (18), 4420–4428.
- Chen, J.J., Yeh, H.H., Tseng, I.C., 2009. Effect of ozone and permanganate on algae coagulation removal: a pilot and bench scale tests. In: *Chemosphere*, 74, pp. 840–846.
- Chow, C.W.K., Drikas, M., Velzeboer, R.M.A., 1999. The impact of conventional water treatment processes on cells of the cyanobacterium *Microcystis aeruginosa*. *Water Res.* 33, 3253–3262.
- Daly, R.I., Ho, L., Brookes, J.D., 2007. Effect of chlorination on *Microcystis aeruginosa* cell integrity and subsequent microcystin release and degradation. *Environ. Sci. Technol.* 41, 4447–4453.
- Ding, J., Shi, H., Adams, C., 2010. Release and removal of microcystins from *Microcystis* during oxidative-, physical-, and UV-based disinfection. *J. Environ. Eng.* 136 (1), 2–11.
- Fan, J., Daly, R., Brookes, J., 2013a. Impact of potassium permanganate on cyanobacterial cell integrity and toxin release and degradation. *Chemosphere* 92, 529–534.
- Fan, J., Ho, L., Brookes, J.D., 2013b. Evaluating the effectiveness of copper sulphate, chlorine, potassium permanganate, hydrogen peroxide and ozone on cyanobacterial cell integrity. *Water Res.* 47, 5153–5164.
- Fan, J., Hobson, P., Brookes, J.D., 2014. The effects of various control and water treatment processes on the membrane integrity and toxin fate of cyanobacteria. *J. Hazard Mater.* 264, 313–322.
- Harke, M.J., Steffen, M.M., Paerl, H.W., 2016. A review of the global ecology, genomics, and biogeography of the toxic cyanobacterium, *Microcystis* spp. *Harmful Algae* 54, 4–20.

- He, X., Liu, Y.L., Walker, H.W., 2016. Toxic cyanobacteria and drinking water: impacts, detection, and treatment. *Harmful Algae* 54, 174–193.
- Ho, L., Onstad, G., Newcombe, G., 2006. Differences in the chlorine reactivity of four microcystin analogues. *Water Res.* 40 (6), 1200–1209.
- Ho, L., Lambling, P., Newcombe, G., 2011. Application of powdered activated carbon for the adsorption of cylindrospermopsin and microcystin toxins from drinking water supplies. *Water Res.* 45 (9), 2954–2964.
- Hyenstrand, P., Metcalf, J., Codd, G., 2001. Effects of adsorption to plastics and solvent conditions in the analysis of the cyanobacterial toxin microcystin-LR by high performance liquid chromatography. *Water Res.* 35 (14), 3508–3511.
- Huang, T., Zhao, J., Chai, B., 2008. Mechanism studies on chlorine and potassium permanganate degradation of microcystin-LR in water using high-performance liquid chromatography tandem mass spectrometry. *Water Sci. Technol.* 58 (5), 1079–1084.
- Jeong, B., Oh, M.S., Hong, S.W., 2017. Elimination of microcystin-LR and residual Mn species using permanganate and powdered activated carbon: oxidation products and pathways. *Water Res.* 114, 189–199.
- Kim, M.S., Lee, H.J., Lee, C., 2018. Oxidation of microcystins by permanganate: pH and temperature-dependent kinetics, effect of DOM characteristics, and oxidation mechanism revisited. *Environ. Sci. Technol.* 52 (12), 7054–7063.
- Laszakovits, J.R., MacKay, A.A., 2019. Removal of cyanotoxins by potassium permanganate: incorporating competition from natural water constituents. *Water Res.* 155, 86–95.
- Laszakovits, J.R., Somogyi, A., MacKay, A.A., 2020. Chemical alterations of dissolved organic matter by permanganate oxidation. *Environ. Sci. Technol.* 54 (6), 3256–3266.
- Liu, B., Qu, F., Bruggen, B., 2017. *Microcystis aeruginosa*-laden water treatment using enhanced coagulation by persulfate/Fe(II), ozone and permanganate: comparison of the simultaneous and successive oxidant dosing strategy. *Water Res.* 125, 72–80.
- Li, L., Shao, C., Gao, N., 2014. Kinetics of cell inactivation, toxin release, and degradation during permanganation of *Microcystis aeruginosa*. *Environ. Sci. Technol.* 48 (5), 2885–2892.
- Li, X., Qiu, D., Yu, X., 2019a. Importance of messenger RNA stability of toxin synthetase genes for monitoring toxic cyanobacterial bloom. *Harmful Algae* 88, 101642.
- Li, X., Qiu, D., Yu, X., 2019b. Evaluation of RNA degradation in pure culture and field *Microcystis* samples preserved with various treatments. *J. Microbiol. Methods* 164, 105684.
- Li, X., Chen, S., Yu, X., 2020a. Comparing the effects of chlorination on membrane integrity and toxin fate of high- and low-viability cyanobacteria. *Water Res.* 177, 115769.
- Li, X., Chen, S., Yu, X., 2020b. Impact of chlorination on cell inactivation and toxin release and degradation of cyanobacteria at development and maintenance stage. *Chem. Eng. J.* 397, 125378.
- Li, L., Zhu, C., Gao, N., 2018. Kinetics and mechanism of *Pseudoanabaena* cell inactivation, 2-MIB release and degradation under exposure of ozone, chlorine and permanganate. *Water Res.* 147, 422–428.
- Ma, M., Liu, R., Jefferson, W., 2012. Effects and mechanisms of pre-chlorination on *Microcystis aeruginosa* removal by alum coagulation: significance of the released intracellular organic matter. *Sep. Purif. Technol.* 86 (15), 19–25.
- Matilainen, A., Gjessing, E.T., Sillanpää, M., 2011. An overview of the methods used in the characterisation of natural organic matter (NOM) in relation to drinking water treatment. *Chemosphere* 83, 1431–1442.
- Mayer, D.G., Bulter, D.G., 1993. Statistical validation. *Ecol. Modell.* 68, 21–32.
- Merel, S., Walker, D., Thomas, O., 2013. State of knowledge and concerns on cyanobacterial blooms and cyanotoxins. *Environ. Int.* 59, 303–327.
- Naceradska, J., Pivokonsky, M., Janda, V., 2017. The impact of pre-oxidation with potassium permanganate on cyanobacterial organic matter removal by coagulation. *Water Res.* 114, 42–49.
- Nicholson, B.C., Rositano, J., Burch, M.D., 1994. Destruction of cyanobacterial peptide hepatotoxins by chlorine and chloramine. *Water Res.* 28, 1297–1303.
- O’Neil, J.M., Davis, T.W., Gobler, C.J., 2012. The rise of harmful cyanobacteria blooms: the potential roles of eutrophication and climate change. *Harmful Algae* 14, 313–334.
- Pearson, L.A., Hisbergues, M., Neilan, B.A., 2004. Inactivation of ABC transporter gene, *mcyH*, results in the loss of microcystin production in the cyanobacterium *Microcystis aeruginosa* PCC 7806. *Appl. Environ. Microbiol.* 70, 6370–6378.
- Plummer, J.D., Edzwald, J.K., 2002. Effects of chlorine and ozone on algal cell properties and removal of algae by coagulation. *J. Water Supply Res. Technol. AQUA* 51, 307–318.
- Rodríguez, E., Majado, M.E., Acero, J.L., 2007a. Oxidation of microcystins by permanganate: reaction kinetics and implications for water treatment. *Water Res.* 41, 102–110.
- Rodríguez, E., Onstad, G.D., Gunten, U., 2007b. Oxidative elimination of cyanotoxins: comparison of ozone, chlorine, chlorine dioxide and permanganate. *Water Res.* 41 (15), 3381–3393.
- Ross, C., Warhurst, B.C., Ochrietor, J.D., 2019. Mesohaline conditions represent the threshold for oxidative stress, cell death and toxin release in the cyanobacterium *Microcystis aeruginosa*. *Aquatic. Toxicol.* 206, 203–211.
- Stewart, R., 1973. Oxidation by permanganate. In: Wiberg, K. (Ed.), *Oxidation in organic chemistry*. Academic Press, New York.
- Tang, M., Krausfeldt, L.E., Wilhelm, S.W., 2018. Seasonal gene expression and the ecophysiological implications of toxic *Microcystis aeruginosa* blooms in Lake Taihu. *Environ. Sci. Technol.* 52 (19), 11049–11059.
- Tillet, D., Dittmann, E., Neilan, B.A., 2000. Structural organization of microcystin biosynthesis in *Microcystis aeruginosa* PCC7806: an integrated peptide-polyketide synthetase system. *Chem. Biol.* 7, 753–764.
- Wert, E.C., Korak, J.A., Rosario-Ortiz, F.L., 2014. Effect of oxidant exposure on the release of intracellular microcystin, MIB, and geosmin from three cyanobacteria species. *Water Res.* 52, 251–259.
- Wang, L., Qiao, J., Gao, N., 2013. Pre-oxidation with KMnO<sub>4</sub> changes extra-cellular organic matter’s secretion characteristics to improve algal removal by coagulation with a low dosage of polyaluminium chloride. *J. Environ. Sci.* 25 (3), 452–459.
- Waldemer, R.H., Tratnyek, P.G., 2006. Kinetics of contaminants degradation by permanganate. *Environ. Sci. Technol.* 40, 1055–1061.
- WHO, 2014. Guidelines for Drinking Water Quality, fourth ed., 8. World Health Organization, Geneva.
- Wilhelm, S.W., Bullerjahn, G.S., McKay, R.M.L., 2020. The complicated and confusing ecology of *Microcystis* blooms. *mBio* 11, e00529–e00540.
- Xie, P., Ma, J., Chen, L., 2013. Comparison of permanganate pre-oxidation and pre-ozonation on algae containing water: cell integrity, characteristics, and chlorinated disinfection byproduct formation. *Environ. Sci. Technol.* 47, 14051–14061.
- Xu, H., Brookes, J., Pei, H., 2019. Impact of copper sulphate, potassium permanganate, and hydrogen peroxide on *Pseudoanabaena galeata* cell integrity, and release and degradation of 2-methylisoborneol. *Water Res.* 157, 64–73.
- Yap, R.K.L., Whittaker, M., Henderson, R.K., 2014. Hydrophobically- associating cationic polymers micro-bubble surface modifiers in dissolved air flotation for cyanobacteria cell separation. *Water Res.* 61, 253–262.
- Zamyadi, A., Fan, Y., Prévost, M., 2013. Chlorination of *Microcystis aeruginosa*: toxin release and oxidation, cellular chlorine demand and disinfection by-products formation. *Water Res.* 47 (3), 1080–1090.